OTX2 loss causes rod differentiation defect in CRX-associated congenital blindness

Jerome E. Roger,[1] Avinash Hiriyanna,[1] Norimoto Gotoh,[1] Hong Hao,[1] Debbie F. Cheng,[1] Rinki Ratnapriya,[1] Marie-Audrey I. Kautzmann,[1] Bo Chang,[2] and Anand Swaroop[1]

[1]Neurobiology-Neurodegeneration and Repair Laboratory, National Eye Institute, NIH, Bethesda, Maryland, USA.
[2]The Jackson Laboratory, Bar Harbor, Maine, USA.

Leber congenital amaurosis (LCA) encompasses a set of early-onset blinding diseases that are characterized by vision loss, involuntary eye movement, and nonrecordable electroretinogram (ERG). At least 19 genes are associated with LCA, which is typically recessive; however, mutations in homeodomain transcription factor *CRX* lead to an autosomal dominant form of LCA. The mechanism of *CRX*-associated LCA is not understood. Here, we identified a spontaneous mouse mutant with a frameshift mutation in *Crx* (*Crx^Rip*). We determined that *Crx^Rip* is a dominant mutation that results in congenital blindness with nonrecordable response by ERG and arrested photoreceptor differentiation with no associated degeneration. Expression of LCA-associated dominant *CRX* frameshift mutations in mouse retina mimicked the *Crx^Rip* phenotype, which was rescued by overexpression of WT CRX. Whole-transcriptome profiling using deep RNA sequencing revealed progressive and complete loss of rod differentiation factor NRL in *Crx^Rip* retinas. Expression of NRL partially restored rod development in *Crx^Rip/+* mice. We show that the binding of homeobox transcription factor OTX2 at the *Nrl* promoter was obliterated in *Crx^Rip* mice and ectopic expression of OTX2 rescued the rod differentiation defect. Together, our data indicate that OTX2 maintains *Nrl* expression in developing rods to consolidate rod fate. Our studies provide insights into *CRX* mutation-associated congenital blindness and should assist in therapeutic design.

Introduction

Inherited retinal degenerative diseases exhibit tremendous clinical and genetic heterogeneity, with almost 200 genes identified so far (Retinal Information Network) (1). In the 19th century, Theodor Leber described the familial nature of a pigmentary retinopathy and congenital blindness (2), now aptly named Leber congenital amaurosis (LCA). LCA encompasses congenital and early-onset retinopathies that account for 5% of inherited blindness and are characterized by vision loss together with nystagmus and nonrecordable rod and cone photoreceptor response by electroretinogram (ERG) (3). At least 19 LCA genes encoding diverse cellular functions, such as intracellular transport, phototransduction, and transcriptional regulation, have been identified so far (4). While LCA is largely recessive, autosomal dominant inheritance is reported for mutations in *CRX* and *IMPDH1* (5–7). Recent success in effective gene-replacement therapy for patients with LCA2, caused by *RPE65* mutations that affect retinoid isomerase activity, underscores the importance of elucidating the molecular basis of disease, functional analysis of associated genes, and relevance of preclinical animal models (8).

During development, distinct neuronal subtypes in the vertebrate retina originate from common pools of progenitor cells in a conserved order of birth, primarily under the control of intrinsic genetic programs (9, 10). The rod and cone photoreceptors constitute over 70% of all cells in the mammalian retina (11, 12). The regulatory mechanisms for generating photoreceptors from retinal progenitors and their subsequent differentiation into unique and functional photon-capturing neurons are slowly being unraveled (13). The homeodomain protein OTX2 is implicated as a key regulator of photoreceptor cell fate and induces the expression of cone-rod homeobox (*Crx*) transcription factor in postmitotic photoreceptor precursors (14–16). While *Otx2* expression decreases in the photoreceptors after birth, *Crx* is suggested to take over as a primary transcriptional regulator and induce the expression of rod differentiation factor, neural retina leucine zipper (*Nrl*), in differentiating rods (17). CRX exhibits an intimate and synergistic relationship with NRL in controlling rod gene regulatory networks (18–22). CRX is also reported to collaborate with RAR-related orphan nuclear receptor β (RORβ) to initiate the expression of S-opsin and other cone genes (23). Surprisingly, the photoreceptor cell fate is unaltered in the *Crx^−/−* retina; yet the expression of phototransduction genes is greatly reduced and no outer segments are formed, leading eventually to retinal degeneration (24). The enigma is that *Crx* is expressed early in newly postmitotic photoreceptor precursors, much before functional maturation; however, its loss of function leads to photoreceptor degeneration. *Crx* is also suggested to be upstream of *Nrl* in the rod transcriptional hierarchy (17, 25, 26); nonetheless, *Nrl* is also expressed in newborn photoreceptors during the final mitosis (27, 28), around the same time as *Crx* (16). In contrast to *Crx*, *Nrl* is both essential and sufficient for determining rod cell fate and rod-specific gene expression (21, 29, 30). We wondered whether *Otx2*, and not *Crx*, initiates *Nrl* expression? The questions pertaining to respective contribution(s) of *Crx* versus *Otx2* in initiating and/or maintaining the expression of *Nrl* and other rod or cone genes have not been directly addressed in vivo.

A range of diverse clinical phenotypes, from cone-rod dystrophy and retinitis pigmentosa to congenital blindness in LCA, associated with *CRX* mutations in humans (5, 6, 31–33) reveal its more complex role in photoreceptor development and/or function than that reflected by *Crx^−/−* mouse phenotype. Even though a strict genotype-phenotype correlation does not exist, a majority
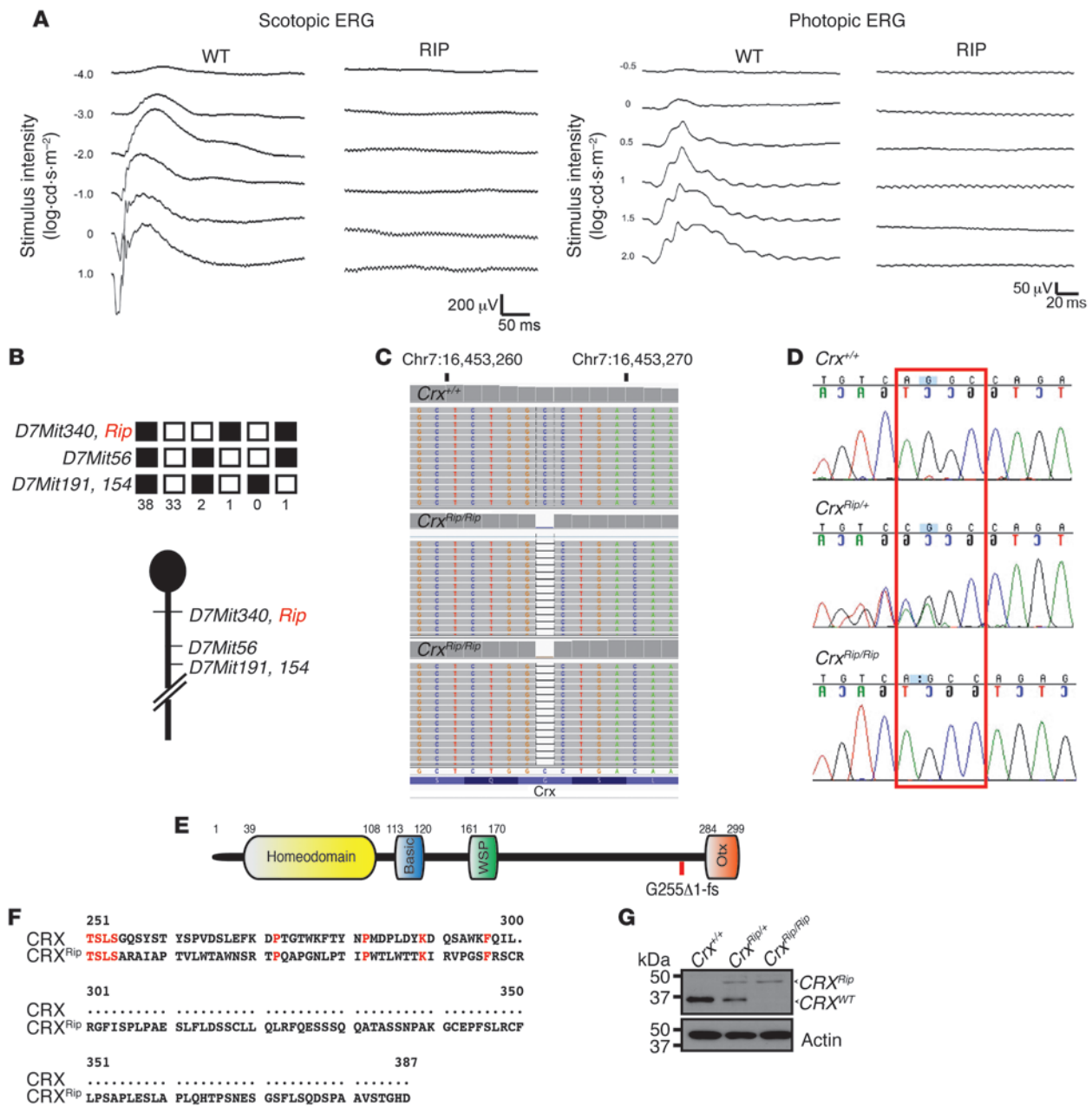
Figure 1
Dominant congenital blindness in the Rip mutant is caused by a 1-bp deletion in *Crx*. (**A**) Dark- and light-adapted ERG recording in 1-month-old WT and *Rip* mutant. (**B**) Linkage cross analysis. 75 backcross progenies from the (Rip mutant X C3A.BLiAPde6b+/J) F1 X C3A.BLiA-Pde6b+/J were phenotyped by retinal fundus examination and genotyped for the indicated microsatellite markers. The black boxes represent heterozygosity for Rip-derived allele, and white boxes represent homozygosity for C3A.BLiA-Pde6b+/J–derived alleles. The number of chromosomes sharing the corresponding haplotype is indicated. Genetic map of chromosome 7 in the Rip region. (**C**) Identification of 1-bp deletion in *Crx*, visualized by Integrative Genome Viewer displaying sequence reads generated by exome capture sequencing. (**D**) Sanger sequencing of *Crx+/+*, *Crx Rip/+*, and *Crx Rip/Rip* mice showing deletion of a G nucleotide in exon 4 in Rip mutant but not WT mice. (**E**) Schematic of the CRX protein, indicating the position of 1-bp deletion upstream of *Otx*-like domain. Colored boxes show the functional domains. (**F**) Alignment of mouse CRX and CRX Rip mutant protein predicts that the frameshift mutation would lead to the addition of 88 amino acids, starting at residue 299. Conserved amino acids are indicated in red. (**G**) Immunoblot analysis of retinal extracts from 1-month-old *Crx+/+*, *Crx Rip/+*, and *Crx Rip/Rip* mice. Anti-CRX antibody identifies 2 CRX bands in *Crx Rip/+* retinas. The lower band (34 kDa) corresponds to CRX WT, whereas the 44-kDa isoforms correspond to CRX Rip protein. Anti-actin antibody was used as a loading control.

Figure 2

Crx^Rip/+ retinas display immature cone-like photoreceptors and long-term preservation of the outer nuclear layer. (**A**) Immunostaining of RHO, OPN1SW, OPN1MW, ARR3, PNA, and Recoverin in P21 *Crx^+/+*, *Crx^Rip/+*, *Crx^Rip/Rip*, and *Crx^–/–* retinas. onl, outer nuclear layer; inl, inner nuclear layer. Scale bar: 40 μm. (**B**) Methacrylate sections followed by H&E staining of retinas from 5-week-, 10-week-, and 9-month-old *Crx^+/+*, *Crx^Rip/+*, *Crx^Rip/Rip*, and *Crx^–/–* mice. rpe, retinal pigment epithelium; os, outer segment; is, inner segment; gcl, ganglion cell layer. Scale bar: 40 μm. (**C**) Methacrylate sections followed by H&E staining in 5-week-old *Crx^+/+*, *Crx^Rip/+*, *Crx^Rip/Rip*, and *Crx^–/–* mice. The arrow indicates characteristic rod photoreceptor nuclei with dense chromatin in the center, and arrowheads indicate characteristic cone photoreceptor nuclei with less condensed chromatin. Scale bar: 10 μm. (**D**) Immunostaining using ribeye and PKCα antibodies to visualize presynaptic photoreceptor region and ON bipolar cells, respectively, in P21 *Crx^+/+* and *Crx^Rip/+* retinas. opl, outer plexiform layer. Scale bar: 40 μm (left); 10 μm (right).
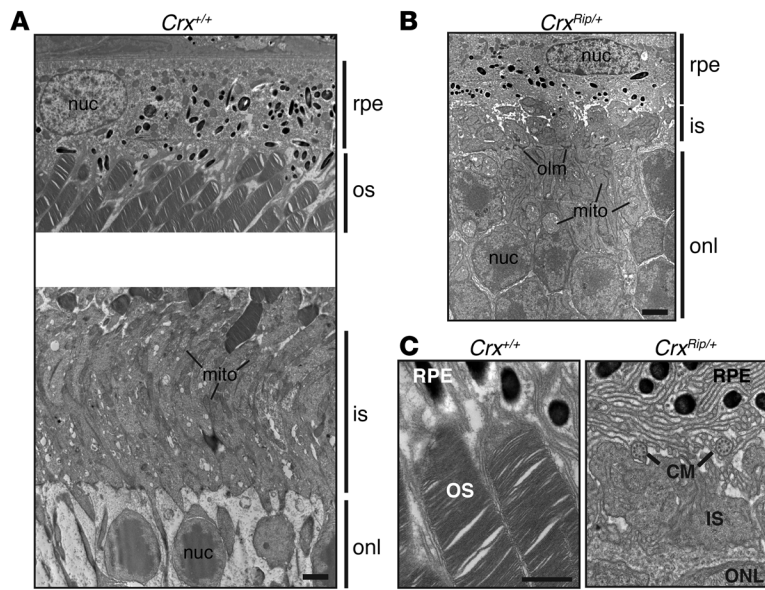
Figure 3
$Crx^{Rip/+}$ retinal photoreceptors lack outer segments and possess very short inner segments. Transmission EM images in the dorsal-ventral midline plane taken through the central retinas of 1-month-old (**A**) $Crx^{+/+}$ and (**B**) $Crx^{Rip/+}$ mice. mito, mitochondria; nuc, nucleus; olm, outer limiting membrane. Original magnification, ×1,200. Scale bar: 2 μm. (**C**) Transmission EM images in the dorsal-ventral midline plane taken through the central retinas of 1-month-old $Crx^{+/+}$ and $Crx^{Rip/+}$ mice, showing the presence of ciliary microtubules in the mutant photoreceptors. CM, ciliary microtubule. Original magnification, ×5,000. Scale bar: 1 μm.

of missense and truncation mutations in the CRX homeodomain are associated with cone-rod dystrophy and alter its DNA binding properties or transcriptional synergy with NRL (34, 35), thereby influencing gene expression and photoreceptor maturation. In contrast, many human *CRX* frameshift mutations identified downstream of the homeodomain result in dominant and more severe LCA phenotypes. The molecular events underlying congenital blindness in CRX retinopathies are poorly understood, and no treatment is currently available.

Here, we demonstrate the molecular mechanism of LCA associated with dominant *CRX* frameshift mutations by taking advantage of a new spontaneous mouse mutant (*Crx^Rip* mice). By combined genetic mapping and exome sequencing, we have identified a 1-bp frameshift deletion in *Crx* coding sequence, similar to many LCA-causing dominant *CRX* mutations (dominant *CRX*-LCA). We show that the CRX^Rip protein, carrying additional unrelated residues at the carboxyl terminus, is not functional in vitro but represses both CRX and OTX2 functions in vivo. LCA-causing *CRX* mutations exhibit phenotypic manifestations similar to those of *Crx^Rip* mice. We demonstrate that the rodless phenotype observed in *Crx^Rip* mutants is caused by the loss of *Nrl* expression later in photoreceptor maturation and can be rescued partially by *Nrl*. ChIP studies reveal that in vivo binding of OTX2 to *Nrl* promoter is abrogated in the *Crx^Rip* mutant retinas but not in the *Crx^-/-* retinas, suggesting that OTX2 is a direct modulator of *Nrl* expression. Our studies thus reveal a critical role of OTX2 in consolidating cell fate by maintaining *Nrl* expression in developing rods. In addition, we establish *Crx^Rip* mutant mice as a preclinical model for dominant *CRX*-LCA and suggest opportunities for gene-based therapies.

Results

Identification of a new mouse mutant with congenital blindness and immature photoreceptors. As part of our systematic screen to identify genetic models of retinal disease, we identified a mouse mutant with white spots on retinal fundus examination. Breeding of this mutant to WT C57BL/6J mice and at least 5 backcrosses revealed an autosomal dominant inheritance of the observed phenotype. Ocular coherence tomography (OCT) Doppler imaging showed smaller retinal blood vessels and poor blood flow in the mutant mice compared with that in the controls (data not shown). Photopic and scotopic ERGs revealed a complete absence of cone and rod visual response, respectively, in 1-month-old heterozygous mutant animals (Figure 1A), suggesting a defect in photoreceptor development. This mutation was hereafter referred to as Rip (retina with immature photoreceptors).

To discover the genetic cause of the Rip mutant phenotype, we performed linkage analysis and identified a locus on chromosome 7 between markers *D7Mit340* and *D7Mit56* (Figure 1B), homologous to human Chr19q13.3. This critical region spanned 17 Mb and contained over 200 genes. We then performed whole-exome sequencing using DNA from 2 homozygous mutant mice, selected by using microsatellite marker haplotypes, and 1 control WT mouse. After mapping the sequence reads, variant calling, and filtering, we identified only 1 homozygous variant that was present in both mutants but was absent in the control. This variant corresponded to a 1-bp deletion in the *Crx* gene at position 763 (c.763del1) and was confirmed by Sanger sequencing (Figure 1, C and D). The c.763del1 mutation, located in the last *Crx* exon, would result in a frameshift that skips the C-terminal Otx-like domain and adds 133 unrelated residues (p.Gly255fs or p.Gly255Alafs*133) (Figure 1, E and F). Immunoblot analysis of adult retina protein extracts, using anti-CRX antibody against an epitope corresponding to the residues 166–285, detected both WT and mutant CRX protein in $Crx^{Rip/+}$ mice (of 34 and 44 kDa, respectively) and only a 44-kDa mutant protein in the $Crx^{Rip/Rip}$ retinas (Figure 1G).

$Crx^{Rip/+}$ mouse retinas display long-term preservation of immature cone-like photoreceptors. We performed a detailed phenotypic analysis of the $Crx^{Rip/+}$ and $Crx^{Rip/Rip}$ retinas and compared it to that of the $Crx^{-/-}$ mice. Immunohistochemical analysis of the mature P21 $Crx^{Rip/+}$ and $Crx^{Rip/Rip}$ retinas showed no rhodopsin (RHO) expression (Figure 2A). In contrast, $Crx^{-/-}$ retinas contained RHO-positive cells, albeit considerably less intensely stained compared with WT retinas. The cone-specific proteins — S-opsin (OPN1SW), M-opsin (OPN1MW), and cone arrestin (ARR3) — were detected in few cells in P21 $Crx^{-/-}$ retinas; however, these markers were completely absent in the $Crx^{Rip/+}$ and $Crx^{Rip/Rip}$ retinas. Furthermore, $Crx^{Rip/+}$ retinas revealed very strong and continuous staining for peanut agglutinin (PNA), a cone-specific cell surface marker, similar to that in $Nrl^{-/-}$ retinas (36, 37). Immunostaining of recoverin, an early marker of photoreceptor differentiation, was also dramatically reduced in $Crx^{Rip/+}$ mice compared with that in WT mice, with only a few recoverin-positive cells in $Crx^{Rip/Rip}$ mutants. In contrast, the expression of recoverin was high but restricted to fewer photoreceptor cells in the $Crx^{-/-}$ retinas.
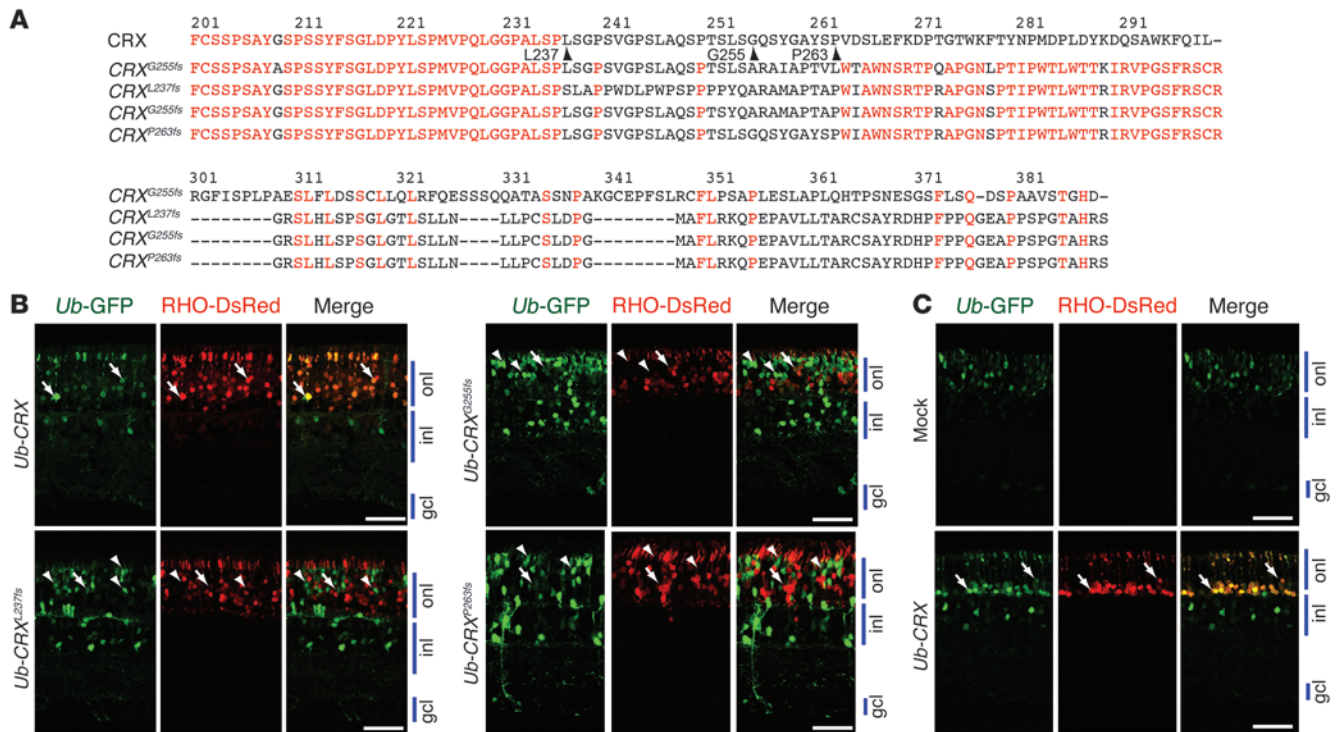
Figure 4

LCA-associated *CRX* frameshift mutations mimic *Crx^Rip* phenotype that can be rescued by *Crx^WT*. (**A**) Alignment of mouse *Crx^G255fs* and the corresponding human mutation *CRX^G255fs* with 2 other human frameshift mutants: *CRX^L237fs* and *CRX^P263fs*. The top line corresponds to human CRX, indicating the degree of conservation between mouse and human. Conserved amino acids are indicated in red. Arrowheads indicate the position of the amino acid changed in *CRX^L237fs*, *Crx^G255fs*, *CRX^G255fs*, and *CRX^P263fs*. (**B**) Representative images of P21 WT mouse retinas electroporated at P0 with *Ub*-GFP (green), *Rho*-DsRed (red), and with one of the following *CRX* frameshift mutants: *CRX^L237fs*, *CRX^G255fs*, or *CRX^P263fs*. *CRX* was used as control. Arrows indicate GFP- and RHO-positive cells, and arrowheads indicate GFP-positive and RHO-negative cells. Scale bar: 40 μm. (**C**) Representative images of P21 *Crx^Rip/+* mouse retinas electroporated at P0 with *Ub*-GFP (green), RHO-DsRed (red), and either CRX^WT or empty vector (Mock). Arrows indicate GFP- and RHO-positive cells. Scale bar: 40 μm.

The histology of 5-week-old retinas in methacrylate sections revealed abnormal photoreceptor segments in the 3 mutants compared with WT mice (Figure 2B). The thickness of outer nuclear layer in *Crx^Rip/+* mice was relatively well preserved at 5 weeks (Figure 2B) and remained largely unchanged, at least up to 18 months, despite the complete loss of visual function (Supplemental Figure 1; supplemental material available online with this article; doi:10.1172/JCI72722DS1). In contrast, the photoreceptor layer in *Crx^Rip/Rip* and *Crx^-/-* retinas underwent rapid degeneration between 5 and 10 weeks, and only a few nuclei persisted at 9 months of age (Figure 2B). The chromatin density and organization of the photoreceptors in *Crx^Rip/+* retinas revealed cone-like characteristics (ref. 38 and Figure 2C), similar to those observed in cone-only *Nrl^-/-* mice (29, 36). This observation is consistent with the complete absence of RHO expression (Figure 2A). Immunohistochemical analysis of the mature P21 *Crx^+/+* and *Crx^Rip/+* retinas using ribeye antibody (a presynaptic marker) and PKCα (to visualize the postsynaptic connection with rod bipolar cells) revealed a certain degree of contact between these two types of cells, even in the absence of visual transduction (Figure 2D). However, neuronal sprouting of the immature photoreceptors into the inner nuclear layer was observed with ribeye staining that was not restricted to the top part of the outer plexiform layer, as in the control retinas. EM of *Crx^Rip/+* mouse retinas confirmed the presence of very short inner segments and a complete absence of

outer segments (Figure 3, A and B), but ciliary microtubules were detectable (Figure 3C). The outer limiting membrane was present in *Crx^Rip/+* retinas, and, unlike the WT photoreceptors, a majority of mitochondria surrounded nuclei instead of being in the distal ellipsoid region (Figure 3, A and B).

Our data demonstrate that *Crx^Rip/+* mutant retinas exhibit a more severe phenotype compared with that of *Crx^-/-* mice, as the immature cone-like photoreceptors do not express many of the key rod or cone phototransduction genes.

LCA-associated CRX frameshift mutations mimic the mouse Crx^Rip phenotype, which can be rescued by WT Crx. The *Crx^Rip* mutation (*CRX^G255fs* refers to the corresponding change in humans) is in a conserved domain of CRX, in close proximity of several similar 1-bp deletion mutations associated with dominant LCA in humans (35). We therefore selected 2 human mutations — *CRX^L237fs* and *CRX^P263fs* (Figure 4A) — to test their effect on photoreceptor development in mouse retina. Neonatal WT mouse retinas were cotransfected in vivo with each *CRX* expression construct, along with *Ub*-GFP and *Rho*-DsRed plasmids (Figure 4B). As predicted, a vast majority of WT CRX–transfected (*CRX^WT*-transfected) cells (GFP-positive) in the outer nuclear layer coexpressed DsRed (*Rho* promoter active) and exhibited elongated outer segments, indicative of rod photoreceptors. However, the transfection of *CRX^G255fs*, *CRX^L237fs*, or *CRX^P263fs* (indicated by GFP) resulted in DsRed-negative cells
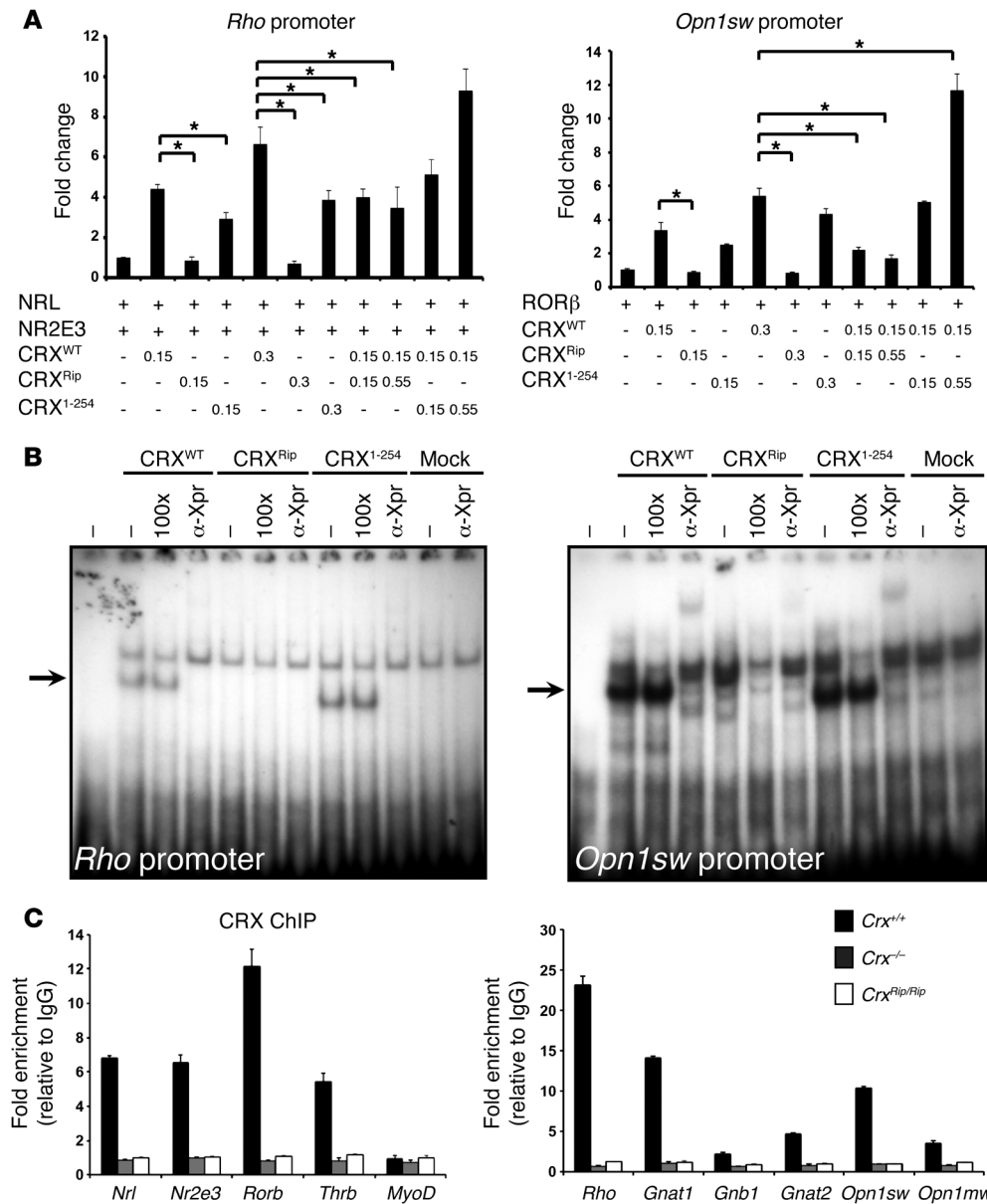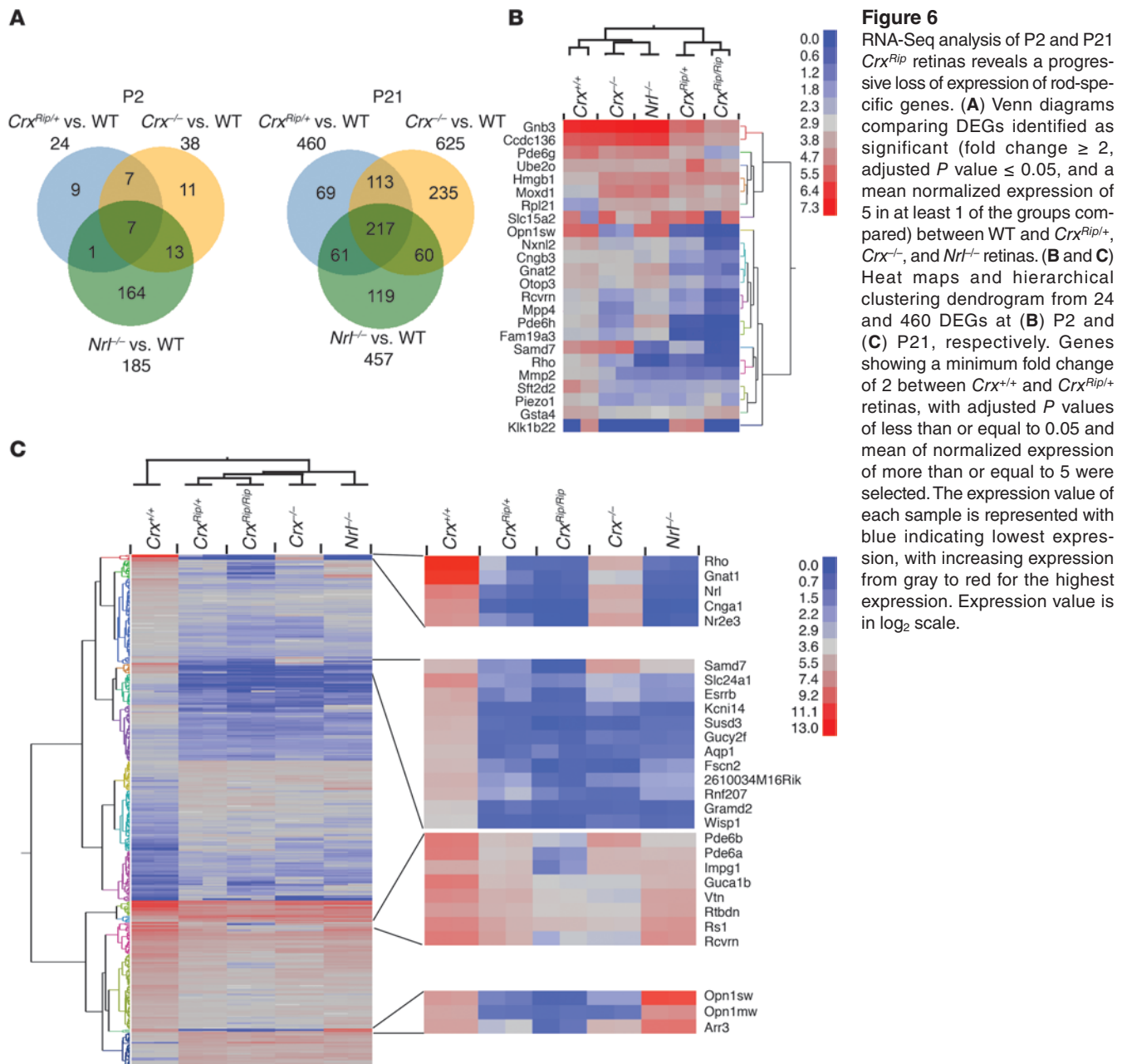
Figure 5
The CRX[Rip] mutant protein is functionally null in vitro. (**A**) Lack of transactivation by CRX[Rip] mutant protein. HEK293 cells were cotransfected with constructs containing bovine *Rho* or mouse *Opn1sw* promoters driving firefly *Luciferase* reporter gene simultaneously with NRL, NR2E3, or RORβ, respectively. In both sets of experiments, different amounts of CRX[WT], CRX[Rip], and/or CRX[1–254] (0.15–0.55 μg) were cotransfected. Fold change is relative to the luciferase activity in presence of *NRL* and *NR2E3* only. *P < 0.05. (**B**) CRX[Rip] protein does not bind DNA. Autoradiograms of EMSA using nuclear extracts from HEK293T cells transfected with pcDNA4c, Xpress-tagged CRX[WT], CRX[Rip], and CRX[1–254] were performed using oligonucleotides encompassing CRX binding sites in *Rho* and *Opn1sw* promoters. 100 times more unlabeled specific probes were used for competition. Oligonucleotide supershift assays were performed with anti-Xpress antibody. Arrows indicate the CRX-shifted probe. (**C**) ChIP-qPCR with anti-CRX antibody from P21 WT, *Crx[Rip/Rip]*, and *Crx^{–/–}* retinas. Normal IgG was used control. Fold enrichment represents the fold change of qPCR amplification signals for the different genes tested between CRX ChIP DNA and IgG control ChIP DNA.

that lacked outer segments. Our data suggest that LCA-associated *CRX* frameshift mutations (caused by 1-bp deletion in the last exon) arrest the committed photoreceptors in an early differentiation state and that the *Crx[Rip/+]* mutant can be used as a model of dominant LCA.

The dominant inheritance of the mutation would imply that the *Crx[Rip]* allele is functionally null, but then why does the *Crx[Rip]* mutant exhibit a dominant retinal phenotype, which is more severe compared with that exhibited by the *Crx^{–/–}* retina, even though WT protein is still present in the *Crx[Rip/+]* retina (see Figure 1G)? We hypothesized that CRX[Rip] mutant protein interferes with the binding of CRX[WT] protein to CRX target genes in vivo. If this were the case, the expression of additional CRX[WT] protein would restore photoreceptor differentiation by blocking the function of the available mutant CRX[Rip] protein. Indeed, the transfection of *CRX[WT]* construct but not of the empty vector in the newborn *Crx[Rip/+]* mouse retina by electroporation in vivo completely amelio-

rated the photoreceptor morphology (including outer segments) and restored RHO expression in rod cells (Figure 4C).

The CRX[Rip] mutant protein does not transactivate opsin promoters or bind DNA. To investigate the mechanism of lack of opsin expression in mutants, we examined the function of CRX[Rip] protein in HEK293 cells using 2 established CRX target promoters — *Rho* and *Opn1sw*. To test *Rho* promoter transactivation, the CRX[WT] or CRX[Rip] construct was cotransfected with two known CRX interactors, NRL and NR2E3, whereas *Opn1sw* promoter activity was evaluated in presence of RORβ, as described previously (22, 23, 39, 40). In contrast to CRX[Rip], the CRX[Rip] mutant protein did not exhibit any transactivation of *Rho* or *Opn1sw* promoter, either alone or with respective coactivators (Figure 5A), even though the protein was produced and localized in the nucleus (Supplemental Figure 2). To test whether the loss of function of CRX[Rip] protein was due to the lack of *Otx*-like domain or unrelated residues at C terminus, we generated a CRX[1–254] expression construct by introducing a non-

Figure 6
RNA-Seq analysis of P2 and P21 *Crx*^Rip retinas reveals a progressive loss of expression of rod-specific genes. (**A**) Venn diagrams comparing DEGs identified as significant (fold change ≥ 2, adjusted *P* value ≤ 0.05, and a mean normalized expression of 5 in at least 1 of the groups compared) between WT and *Crx*^Rip/+, *Crx*^-/-, and *Nrl*^-/- retinas. (**B** and **C**) Heat maps and hierarchical clustering dendrogram from 24 and 460 DEGs at (**B**) P2 and (**C**) P21, respectively. Genes showing a minimum fold change of 2 between *Crx*^+/+ and *Crx*^Rip/+ retinas, with adjusted *P* values of less than or equal to 0.05 and mean of normalized expression of more than or equal to 5 were selected. The expression value of each sample is represented with blue indicating lowest expression, with increasing expression from gray to red for the highest expression. Expression value is in log₂ scale.

sense mutation in Gly255 codon. The truncated CRX^1–254 protein was able to transactivate both *Rho* and *Opn1sw* promoters, albeit less efficiently compared with CRX^WT. Additional cotransfection experiments revealed that increasing amounts of CRX^Rip construct (0.15–0.55 μg) did not alter the activity of CRX^WT (kept constant at 0.15 μg), whereas transcriptional activation of opsin promoters was further augmented by CRX^1–254 (Figure 5A). Our results show that *Otx2*-like C-terminal domain of CRX is not critical for transcriptional activation and that the CRX^Rip mutant does not act as a dominant-negative suppressor of the CRX^WT protein or other coactivators (NRL, NR2E3, or RORβ) in cultured cells.

To examine why CRX^Rip protein does not transactivate in reporter assays, we performed electrophoretic mobility shift experiments with *Rho* and *Opn1sw* promoter elements (both encompass-ing CRX binding sites) using nuclear extracts from transfected cells (Figure 5B). As predicted, CRX^WT and CRX^1–254 proteins shifted the mobility of the 2 promoter elements, but the CRX^Rip protein did not bind cognate CRX binding sites. In concordance, ChIP-qPCR analysis of P21 retinas from *Crx*^Rip/Rip and *Crx*^-/- (as control) mice using anti-CRX antibody showed no CRX binding to photoreceptor-specific target genes (Figure 5C). We conclude that the lack of transcriptional activity by CRX^Rip is a consequence of the loss of DNA binding.

RNA-Seq analysis of Crx^Rip mutant retinas, unlike that of Crx^-/- ret-inas, reveals a complete lack of phototransduction gene expression. To gain additional molecular insights, we performed whole-tran-scriptome sequencing (using RNA sequencing [RNA-Seq]; ref. 41) of P2 (corresponding to the peak of rod birth) and mature (P21)

Table 1

Total number of DEGs at P2 and P21 identified as significant between each mouse mutant

P2	Crx^Rip/+	Crx^Rip/Rip	Crx^−/−	Nrl^−/−
Crx^+/+	24	69	38	185
Crx^Rip/+		28	27	165
Crx^Rip/Rip			60	178
Crx^−/−				99
P21	**Crx^Rip/+**	**Crx^Rip/Rip**	**Crx^−/−**	**Nrl^−/−**
Crx^+/+	460	623	625	457
Crx^Rip/+		167	216	203
Crx^Rip/Rip			273	398
Crx^−/−				368

The DEGs were filtered based on the following criteria: fold change of more than or equal to 2, adjusted P value of less than or equal to 0.05, and a mean of normalized expression of 5 in at least one of the groups compared.

$Crx^{Rip/+}$ and $Crx^{Rip/Rip}$ retinas (Figure 6). In addition, we included WT ($Crx^{+/+}$), $Crx^{−/−}$, and $Nrl^{−/−}$ retinas for comparative analysis. We used a cutoff of fold change of 2, FPKM (fragments per kilobase of exon per million fragments mapped) value of more than or equal to 2, and an adjusted P value of less than or equal to 0.05 to identify differentially expressed genes (DEGs) at P2 and P21 among different pairwise combinations. As shown in Supplemental Figure 3, volcano plots show the distinctions in gene expression patterns of retinas from various mutants. Only 24 genes were differentially expressed between $Crx^{Rip/+}$ and WT retinas at P2, but many more genes showed differential expression at P21 (Figure 6A and Table 1). Two-way hierarchical clustering of DEGs using a higher normalized FPKM cutoff of 5 revealed divergent gene expression patterns in P2 Rip mutant retinas when compared with corresponding $Crx^{+/+}$, $Crx^{−/−}$, and $Nrl^{−/−}$ retinas (Figure 6B); however, the expression profiles of Crx^{Rip} mutants at P21 were more similar to $Crx^{−/−}$ retinas then $Nrl^{−/−}$ retinas, relative to WT controls (Figure 6C).

In general, unlike that in $Crx^{−/−}$ and $Nrl^{−/−}$ retinas, the expression of a majority of photoreceptor genes needed for visual transduction was completely undetectable in the $Crx^{Rip/+}$ and $Crx^{Rip/Rip}$ mutants. Notable exceptions were a subset of cone-specific genes (such as $Gnb3$, $Gnat2$, $Pde6c$, and $Cngb3$) that were downregulated at P2 but upregulated in P21 $Crx^{Rip/+}$ retinas (Figure 6C and Supplemental Table 1). In contrast, the expression of these genes was upregulated or unchanged at P2 in $Crx^{−/−}$ retinas.

The pathway analysis of 69 genes showing differential expression between P21 $Crx^{Rip/+}$ and $Crx^{+/+}$ retinas, but unaltered expression in $Crx^{−/−}$ or $Nrl^{−/−}$ retinas, highlights several cell death and survival genes, including $Stat3$, that are associated with neuroprotection as well as suppression of rod differentiation (Supplemental Figure 4 and refs. 42, 43). These data are consistent with the preservation of outer nuclear layer in $Crx^{Rip/+}$ mutants, with a concurrent lack of photoreceptor maturation.

Nrl can partially rescue the rod phenotype in $Crx^{Rip/+}$ retinas. A key finding from RNA-seq analysis was that, unlike $Crx^{−/−}$ retinas, the expression of rod differentiation factor Nrl was detectable in P2 but not P21 $Crx^{Rip/+}$ retinas (Figure 6, B and C, and Supplemental Table 1). A complete absence of rod gene expression (including $Nr2e3$, $Mef2c$, Rho, and other phototransduction genes) in mature retina

can thus be explained simply by the loss of NRL (21). Immunoblot analysis and qPCR analysis showed that the expression of NRL was dramatically reduced after P6 in $Crx^{Rip/+}$ mutant retinas and was absent at and after P14, whereas NRL expression in $Crx^{−/−}$ retinas decreased at a much slower rate (Figure 7A and Supplemental Figure 5). We hypothesized that the loss of NRL at or immediately after P6 would not permit immature committed precursors to complete the rod differentiation program. To test this hypothesis, we maintained Nrl expression independent of its own promoter by mating Crx^{Rip} mutants with $Crxp::Nrl$ mice, in which Nrl expression is driven by the Crx promoter (active in the Crx^{Rip} mutant) in all photoreceptor precursors leading to rod-only retina (30). Scotopic ERG recordings revealed a partial rescue of the rod function in $Crxp::Nrl;Crx^{Rip/+}$ retinas, with shorter outer segments expressing RHO and peripherin and with nuclei displaying a rod-like denser chromatin (Figure 7, B–D). As predicted, no cone-mediated photopic ERG response was detectable (data not shown). The expression of Nrl and $Nr2e3$ (completely absent in Rip mutants) was restored by $Crxp::Nrl$ transgene, with no effect on Crx expression (Figure 7E). The rod-specific transcriptional targets of NRL, including Rho, $Gnat1$, $Cnga1$, and $Esrrb$ (21), were expressed in $Crxp::Nrl;Crx^{Rip/+}$ retinas, but cone genes (such as $Arr3$) remained undetectable. Notably, ectopic Nrl expression did not prevent photoreceptor degeneration in the $Crxp::Nrl;Crx^{Rip/Rip}$ retinas, presumably because of the strong inhibitory effect of the mutant protein or complete absence of the CRX^WT (data not shown). Our data showing the partial rescue of the rod phenotype in $Crx^{Rip/+}$ retinas by ectopic Nrl expression suggested that Crx^{Rip} allele did not block NRL function.

Otx2 binds to promoters of rod genes, including Nrl, in WT and $Crx^{−/−}$ retinas, but not in $Crx^{Rip/Rip}$ retinas, and it can restore Rho expression. The presence of homeodomain binding sites in the Nrl promoter (17, 44) would argue in favor of CRX and/or OTX2 being the major regulators of Nrl. However, as Nrl expression is rapidly turned off in $Crx^{Rip/+}$ mutants compared with that in $Crx^{−/−}$ mice, we propose that OTX2, and not CRX, is a major contributor for the initiation or maintenance of Nrl transcription in developing retinas. Indeed, RNA-Seq analysis (Supplemental Table 1) showed a small but statistically significant ($P < 0.001$) increase of $Otx2$ expression in $Crx^{Rip/+}$, $Crx^{Rip/Rip}$, and $Crx^{−/−}$ retinas (1.6-, 2.9-, and 2.1-fold, respectively), indicating that OTX2 might compensate for the lack of CRX, as demonstrated in *Drosophila* (45). In addition, transcriptome analysis of flow-sorted WT mouse rod photoreceptors at P2 and P21 revealed continued (though reduced) expression of $Otx2$ (Table 2).

To further test the potential role of OTX2 in developing and mature retina, we performed OTX2 ChIP-qPCR analysis (Figure 8A). Indeed, the promoters of Nrl and several rod-specific genes exhibited OTX2 binding in P21 WT and $Crx^{−/−}$ retinas; however, the binding of OTX2 to its target genes was completely abrogated in the $Crx^{Rip/Rip}$ retinas (Figure 8A). Additionally, OTX2 binding to the cone-specific promoters was observed in WT and $Crx^{−/−}$ retinas but not in the $Crx^{Rip/Rip}$ mutant retinas. Our results argue strongly in support of the lack of OTX2 binding being the primary mechanism for the loss of both rod and cone gene expression in the Rip mutants.

Based on the dominant phenotype and lack of OTX2 binding to rod and cone gene promoters in the $Crx^{Rip/Rip}$ retinas, we wondered whether overexpression of OTX2 could rescue the $Crx^{Rip/+}$ mutant phenotype. In vivo transfection of Ub-GFP (GFP expression identifies the electroporated cells) with Ub-$OTX2$ construct in retinas of newborn $Crx^{Rip/+}$ mice demonstrated that by P21 a vast majority of $Otx2$-positive cells (and none of the mock-transfected cells)
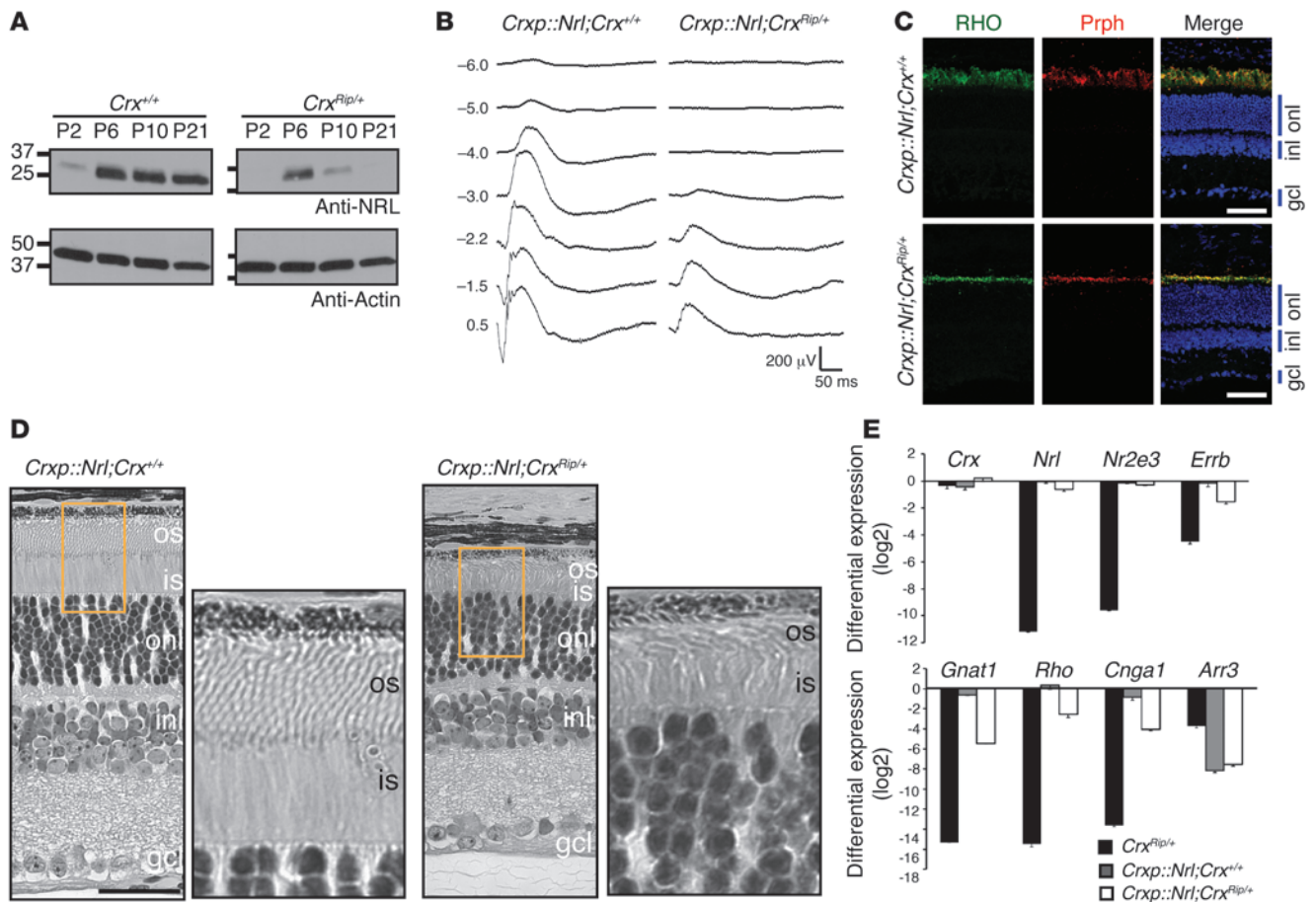
Figure 7

Expression of NRL partially rescues the Rip mutant phenotype. (**A**) Immunoblot analysis using retinal extracts from P2, P6, P10, P21 *Crx+/+* and *CrxRip/+* mouse retinas that were probed with anti-NRL antibody. Anti-actin antibody was used as a loading control. (**B**) Dark-adapted ERG recording in 1-month-old *Crxp::Nrl;Crx+/+* and *Crx::Nrl;CrxRip/+* mice. (**C**) Immunolabeling analysis of RHO (green) and peripherin (red) in 1-month-old *Crxp::Nrl;Crx+/+* and *Crxp::Nrl;CrxRip/+* mice. Scale bar: 40 μm. (**D**) Methacrylate sections followed by H&E staining on 1-month-old *Crxp::Nrl;Crx+/+* and *Crxp::Nrl;CrxRip/+* mice. Scale bar: 40 μm. (**E**) Differential expression analysis by qPCR of photoreceptor transcription factors (*Crx*, *Nrl*, *Nr2e3*, *Err*) and genes involved in rod (*Gnat1*, *Rho*, *Cnga1*) or cone (*Arr3*) phototransduction. For each gene, all values were expressed as mean ± SEM from 3 biological replicates and compared to mRNA expression of WT mice after normalizing by the average expression of 2 housekeeping genes: *Act* and *Hprt*.

expressed RHO (Figure 8B). We conclude that ectopic expression of OTX2 in *CrxRip/+* mouse retinas could activate the *Rho* promoter and should be able to rescue the mutant photoreceptor phenotype.

Discussion

Developmental and/or degenerative diseases affecting retinal photoreceptors are a major cause of inherited visual dysfunction and are largely incurable. While cones dominate visual transduction in humans because of their role in mediating day light and color vision, rods represent 95% of the photoreceptors in the human retina and are affected first in the majority of retinal and macular diseases. A better understanding of regulatory networks that establish rod and cone photoreceptor mosaic in developing retina would be valuable for designing knowledge-based strategies for treatment of congenital blinding diseases, such as LCA. OTX2, CRX, and NRL are key transcriptional regulators guiding rod and cone differentiation. Here, we determine a direct role of OTX2 in initiating and maintaining the transcription of *Nrl* in developing rod photoreceptors by taking advantage of a newly discovered mouse mutant

carrying a *Crx* frameshift mutation. The CRX^Rip protein acts in a dominant-negative manner in vivo and blocks both CRX and OTX2 in postmitotic precursors, consequently producing a more severe phenotype than the loss of CRX alone (as in *Crx–/–* retina). Our studies also provide the mechanism of congenital blindness in patients with LCA carrying dominant *CRX* mutations.

The dominant *CrxRip/+* mutant presents a surprising retinal phenotype, with long-term preservation of functionally inactive and immature photoreceptors that display a decondensed chromatin in the nuclei. The cone-like appearance, but without the expression of either cone or rod visual pigment in *CrxRip/+* photoreceptors, suggests an early block in the developmental pathway before the decision to become a rod or a cone is finalized, consistent with the proposed model of S-cone being the default photoreceptor cell fate (13). We can now extend the model and propose a novel role of OTX2 in rod differentiation (Figure 9). OTX2, and probably CRX, induces the expression of *Nrl* (likely in collaboration with RORβ; refs. 44, 46), which competes with Trβ2 to drive the postmitotic precursors to rod fate (28). We propose that OTX2 is needed in

Table 2
Normalized expression values of *Otx2*, *Crx*, *Nrl*, and *Nr2e3* in whole WT retinas or flow-sorted photoreceptors obtained by whole-transcriptome analysis using RNA-Seq

Gene	Whole retina		Flow-sorted photoreceptors	
	P2	P21	P2	P21
Otx2	329	81	543	73
Crx	204	347	519	577
Nrl	75	447	379	2540
Nr2e3	132	211	544	680

developing rods to maintain *Nrl* levels and that the CRX[Rip] protein inhibits OTX2 binding to *Nrl* promoter thereby blocking rod differentiation. *Crx*^{-/-} data (this report, refs. 16, 20, 26) show that CRX does not affect *Nrl* expression appreciably in early developing rods but rather enhances the expression of phototransduction genes synergistically with NRL to produce mature and functional rods. In the absence of CRX, OTX2 can maintain NRL levels, allowing rod development to proceed, though dramatically reduced expression of RHO and other phototransduction genes does not permit outer segment formation. In concordance, the *Crxp::Nrl* transgene was able to only partially rescue the rod phenotype in *Crx*[Rip/+] mutant retinas, as reflected by ERG and low expression of phototransduction genes (see Figure 7). In *Crx*[Rip/+] retinas, the mutant protein acts as a dominant negative and blocks OTX2, leading to the loss of of both CRX and NRL function and arrest of photoreceptor differentiation. Our P2 RNA-Seq data clearly establish the role of OTX2 in inducing and maintaining NRL expression in developing rods.

In humans, almost 50 *CRX* mutations have been identified in patients with retinopathy (35); a majority of these are fully pene-

trant and act in a dominant manner (47, 48). The *p.G255fs* mutation in *Crx*[Rip] mice (as in several dominant LCA patients) removes the C-terminal *Otx*-like domain of CRX and instead adds 133 unrelated residues. As the truncated CRX[1–254] protein retains DNA binding and transactivation properties consistent with a previous study of CRX functional domains (49), the addition of unrelated residues in CRX[Rip] protein must interfere with the function of CRX[WT] and OTX2 proteins (as discussed earlier). As two dominant LCA-causing mutations examined here mimic the *Crx*[Rip/+] phenotype, our studies provide a plausible molecular mechanism for congenital blindness in dominant CRX-LCA.

The long-term preservation of immature and dysfunctional cones in *Crx*[Rip/+] mutant retinas in the absence of rod photoreceptors is consistent with our recent studies (37, 50) and provides opportunities for elucidating cone survival pathways and designing treatment paradigms for degenerating retinal diseases. At this stage, it is unclear whether dominant *CRX* frameshift mutations arrest photoreceptor differentiation in humans, as disease onset is very early and OCT studies are difficult to perform. Where OCT was possible, significant retinal thinning is observed with some preservation of photoreceptors (34). We believe that *Crx*[Rip/+] mutant mice would serve as reasonable model for assessing gene- or cell-based intervention approaches for dominant *CRX*-LCA. Though disease rescue using AAV-based vectors that express CRX, OTX2, or NRL in target cells may be achievable, the selected gene would have to be introduced very early in infancy. Preliminary investigations of injecting AAV constructs expressing *Nrl* in 2-month-old *Crx*[Rip/+] retinas revealed promising findings, as some RHO expression was restored in photoreceptors (see Supplemental Figure 6). However, more detailed clinical analysis of patients would be clearly desirable to design therapeutic strategies.

We also note that *Crx*^{-/-} mice have been used previously for evaluating cell replacement therapy by photoreceptor transplantation
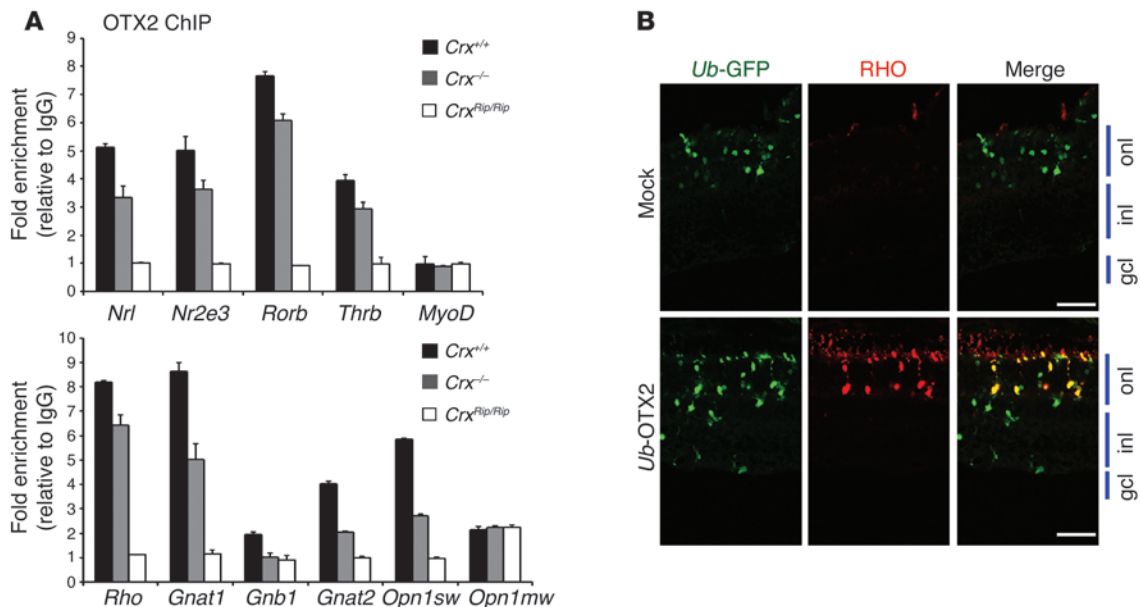

Figure 8
OTX2 binds to promoters of rod genes, including *Nrl*, in WT and *Crx*^{-/-} retinas but not in *Crx*[Rip/Rip] retinas. (**A**) ChIP-qPCR with anti-OTX2 antibody from P21 WT, *Crx*[Rip/Rip], and *Crx*^{-/-} retinas. Normal IgG was used as control. Fold enrichment represents the fold change of qPCR amplification signals for the different genes tested between OTX2 ChIP DNA and IgG control ChIP DNA. (**B**) Representative images of P21 *Crx*[Rip/+] mouse retinas electroporated at P0 with RHO-DsRed (red) and either OTX2-GFP or *Ub*-GFP (green; mock). Scale bar: 40 μm.
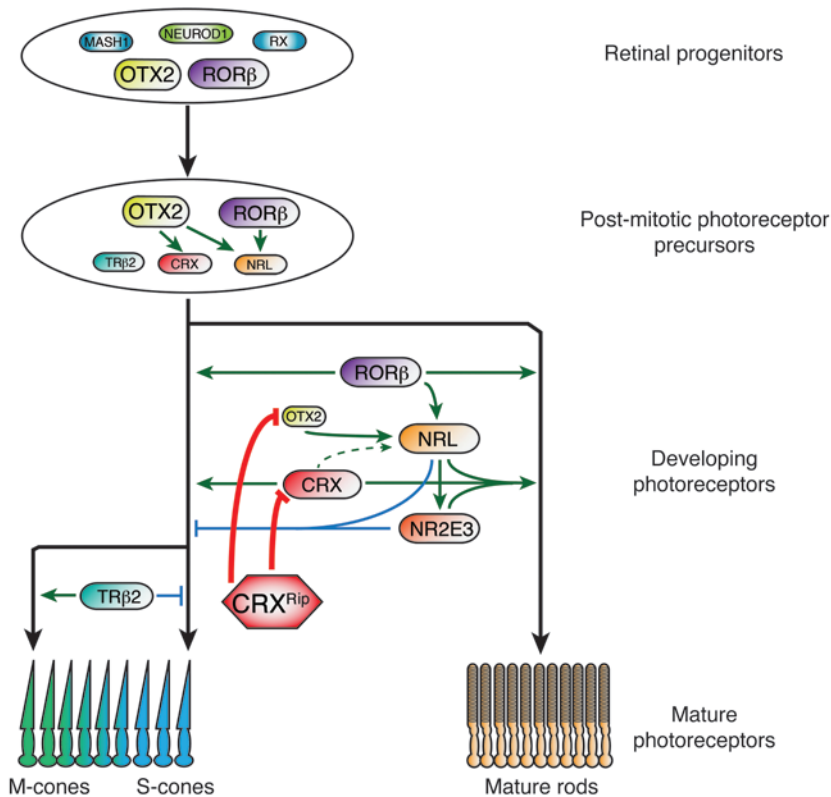
Figure 9
The molecular mechanism of congenital blindness caused by dominant *CRX* frameshift mutations. After cell cycle exit, and under the control of OTX2, postmitotic precursors get restricted to the photoreceptor lineage and are fated to produce both rods and cones. These precursors will differentiate by default into S-cones, unless their fate is directed into rods by the expression of NRL, or into M-cones by the expression of TRβ2. In developing photoreceptors, NRL expression is initiated by OTX2 and RORβ and increases during development to restrict the lineage to rods. OTX2 plays a crucial role in maintaining NRL expression to consolidate rod cell fate. Sustained expression of NRL is needed to induce downstream targets, including NR2E3, that are critical for suppressing cone genes and for rod maturation in collaboration with CRX. In *Crx^Rip/+* mutant retinas, CRX^Rip protein blocks both OTX2 and CRX, arresting NRL expression and, consequently, rod differentiation pathway. In addition, CRX^Rip protein prevents the CRX^WT protein from forming requisite transcriptional complexes for rod gene expression. Ultimately, the arrest in photoreceptor development does not permit phototransduction, causing congenital blindness.

(51, 52); however, photoreceptor cell death occurring in the *Crx^−/−* host retinas may impair long-term survival of the transplanted cells. The unique phenotype of the *Crx^Rip/+* mutant should provide a better host retinal environment for exploring photoreceptor integration and functional assessment in cell replacement therapy.

Methods

Animals and tissue collection. The Rip mutant was identified in C57BL/6J background from our mouse colony by fundus examination. The *Nrl^−/−*, *Crx^−/−*, and *Crxp::Nrl* mice in C57BL/6J background have been described previously (24, 29, 30). Neonatal CD1 mice (Charles River Laboratories) were used for in vivo electroporation. P0 is considered the day of birth. Mice of either sex were used for the study and euthanized by CO_2 inhalation. The procedures for tissue preparation for cryopreservation, methacrylate sections, and RNA/protein extraction have been described earlier (37, 53), and additional details are provided in the Supplemental Methods.

Antibodies. The antibodies used in this study are listed in Supplemental Table 2.

Plasmid constructions and site-directed mutagenesis. The details of cDNA constructs used in this study are described in the Supplemental Methods.

Retinal phenotyping. Mice were anesthetized with ketamine and xylazine. Pupils were dilated using topical 0.5% tropicamide and 1% cyclopentolate hydrochloride. The methods for fundus examination, OCT imaging, and ERG have been described previously (37).

Linkage analysis of Rip mutant mice. We mated *Rip* mutant mice in the C57BL/6J background with C3A.BLiA-Pde6b+/J mice. For linkage analysis, 75 backcross progenies from the (Rip mutant X C3A.BLiAPde6b+/J)F1 X C3A.BLiA-Pde6b+/J were phenotyped by retinal fundus examination and genotyped using microsatellite markers. Genetic markers defining the critical domain were *D7Mit340*, *D7Mit56*, and *D7Mit191*, spanning a 19.5-Mb genomic region.

Exome sequencing and variant calling. Exome capture and sequencing were performed as described previously (54). Genomic DNA (3 μg) from 2 homozygous *Rip* mutants, identified by using the linked markers, and 1 WT mouse was sheared using a Covaris ultrasonicator and subjected to library preparation and whole-exome capture using the SureSelect Human All Exon 50 Mb Kit (Agilent Technologies), following the manufacturer's instructions. The captured libraries were amplified and converted to clusters using Cluster Station. Single-end sequencing was performed on Illumina GAIIx. The sequence reads were mapped to the mouse genome (NCBI37/mm9) using the Burrows-Wheeler Alignment tool (55). Variants were subsequently called using SAMtools (56), and annotations were obtained using ANNOVAR (57).

Immunoblotting and immunohistochemistry. Frozen retinas were lysed by sonication in radioimmunoprecipitation assay buffer supplemented with protease inhibitors (Roche Applied Science). The supernatant proteins were resolved by SDS-PAGE under reducing conditions and transferred to polyvinyl difluoride membrane, as previously described (53). Cryosections were probed with selected antibodies (58). Fluorescent staining signals were captured using an Olympus FluoView FV1000 confocal laser-scanning unit (Olympus America Inc.).

In vivo electroporation in mouse retinas. The retinas of newborn CD1 and Rip mutant mice were electroporated as previously described (53, 59).

EMSAs. EMSAs were performed as previously described (60). The method used for this study is described in the Supplemental Methods.

ChIP-qPCR. ChIP using CRX or OTX2 antibody and normal IgG control was performed as described previously (21) using retinas from P21 WT C57BL/6J, *Crx^−/−*, and *Crx^Rip/Rip* mice. Duplicate ChIP was performed, and the ChIP DNA was quantified by real-time qPCR using SYBR Green Super mixture (Bio-Rad) with the primers listed in Supplemental Table 3.

Whole-transcriptome sequencing (RNA-Seq) and data analysis. RNA extraction, library preparation, and sequencing are detailed in the Supplemental Methods. RNA-seq data are available at GEO (accession no. GSE52006).

Statistics. Two-way comparisons in Figure 5A used 2-tailed Student's *t* tests, and *P* values of less than 0.05 were considered significant. For RNA-seq data, differential expression analysis was performed using DESeq, and an adjusted *P* value of less than or equal to 0.05 was considered significant. Data in Figure 5, A and C; Figure 7E; and Figure 8A are represented using mean ± SEM.

Study approval. All experiments with mice followed the animal protocol approved by the Animal Care and Use Committee of the National Eye Institute, conforming to the Association for Research in Vision and Ophthalmology guidelines.

Acknowledgments

Address correspondence to: Anand Swaroop, N-NRL, National Eye Institute, National Institutes of Health, MSC0610, 6 Center Drive, Bethesda, Maryland, USA. Phone: 301.435.5754; Fax: 301.480.9917; E-mail: swaroopa@nei.nih.gov.

1. Wright AF, Chakarova CF, Abd El-Aziz MM, Bhattacharya SS. Photoreceptor degeneration: genetic and mechanistic dissection of a complex trait. *Nat Rev Genet.* 2010;11(4):273–284.
2. Leber T. Über Retinitis pigmentosa und angeborene Amaurose. *Archiv für Ophthalmologie.* 1869; 15:1–25.
3. Traboulsi EI. The Marshall M. Parks memorial lecture: making sense of early-onset childhood retinal dystrophies — the clinical phenotype of Leber congenital amaurosis. *Br J Ophthalmol.* 2010;94(10):1281–1287.
4. den Hollander AI, Roepman R, Koenekoop RK, Cremers FP. Leber congenital amaurosis: genes, proteins and disease mechanisms. *Prog Retin Eye Res.* 2008;27(4):391–419.
5. Freund CL, et al. De novo mutations in the CRX homeobox gene associated with Leber congenital amaurosis. *Nat Genet.* 1998;18(4):311–312.
6. Sohocki MM, et al. A range of clinical phenotypes associated with mutations in CRX, a photoreceptor transcription-factor gene. *Am J Hum Genet.* 1998; 63(5):1307–1315.
7. Bowne SJ, et al. Spectrum and frequency of mutations in IMPDH1 associated with autosomal dominant retinitis pigmentosa and leber congenital amaurosis. *Invest Ophthalmol Vis Sci.* 2006;47(1):34–42.
8. Cideciyan AV. Leber congenital amaurosis due to RPE65 mutations and its treatment with gene therapy. *Prog Retin Eye Res.* 2010;29(5):398–427.
9. Cayouette M, Barres BA, Raff M. Importance of intrinsic mechanisms in cell fate decisions in the developing rat retina. *Neuron.* 2003;40(5):897–904.
10. Agathocleous M, Harris WA. From progenitors to differentiated cells in the vertebrate retina. *Annu Rev Cell Dev Biol.* 2009;25:45–69.
11. Jeon CJ, Strettoi E, Masland RH. The major cell populations of the mouse retina. *J Neurosci.* 1998; 18(21):8936–8946.
12. Wikler KC, Rakic P. Distribution of photoreceptor subtypes in the retina of diurnal and nocturnal primates. *J Neurosci.* 1990;10(10):3390–3401.
13. Swaroop A, Kim D, Forrest D. Transcriptional regulation of photoreceptor development and homeostasis in the mammalian retina. *Nat Rev Neurosci.* 2010;11(8):563–576.
14. Nishida A, et al. Otx2 homeobox gene controls retinal photoreceptor cell fate and pineal gland development. *Nat Neurosci.* 2003;6(12):1255–1263.
15. Omori Y, et al. Analysis of transcriptional regulatory pathways of photoreceptor genes by expression profiling of the Otx2-deficient retina. *PLoS One.* 2011;6(5):e19685.
16. Muranishi Y, et al. Gene expression analysis of embryonic photoreceptor precursor cells using BAC-Crx-EGFP transgenic mouse. *Biochem Biophys Res Commun.* 2010;392(3):317–322.
17. Montana CL, et al. Transcriptional regulation of neural retina leucine zipper (Nrl), a photoreceptor cell fate determinant. *J Biol Chem.* 2011; 286(42):36921–36931.
18. Chen S, et al. Crx, a novel Otx-like paired-homeodomain protein, binds to and transactivates photoreceptor cell-specific genes. *Neuron.* 1997; 19(5):1017–1030.
19. Furukawa T, Morrow EM, Cepko CL. Crx, a novel otx-like homeobox gene, shows photoreceptor-specific expression and regulates photoreceptor differentiation. *Cell.* 1997;91(4):531–541.
20. Corbo JC, et al. CRX ChIP-seq reveals the cis-regulatory architecture of mouse photoreceptors. *Genome Res.* 2010;20(11):1512–1525.
21. Hao H, et al. Transcriptional regulation of rod photoreceptor homeostasis revealed by in vivo NRL targetome analysis. *PLoS Genet.* 2012; 8(4):e1002649.
22. Mitton KP, Swain PK, Chen S, Xu S, Zack DJ, Swaroop A. The leucine zipper of NRL interacts with the CRX homeodomain. A possible mechanism of transcriptional synergy in rhodopsin regulation. *J Biol Chem.* 2000;275(38):29794–29799.
23. Srinivas M, Ng L, Liu H, Jia L, Forrest D. Activation of the blue opsin gene in cone photoreceptor development by retinoid-related orphan receptor beta. *Mol Endocrinol.* 2006;20(8):1728–1741.
24. Furukawa T, Morrow EM, Li T, Davis FC, Cepko CL. Retinopathy and attenuated circadian entrainment in Crx-deficient mice. *Nat Genet.* 1999; 23(4):466–470.
25. Hsiau TH, Diaconu C, Myers CA, Lee J, Cepko CL, Corbo JC. The cis-regulatory logic of the mammalian photoreceptor transcriptional network. *PLoS One.* 2007;2(7):e643.
26. Hennig AK, Peng GH, Chen S. Regulation of photoreceptor gene expression by Crx-associated transcription factor network. *Brain Res.* 2008;1192:114–133.
27. Akimoto M, et al. Targeting of GFP to newborn rods by Nrl promoter and temporal expression profiling of flow-sorted photoreceptors. *Proc Natl Acad Sci U S A.* 2006;103(10):3890–3895.
28. Ng L, Lu A, Swaroop A, Sharlin DS, Swaroop A, Forrest D. Two transcription factors can direct three photoreceptor outcomes from rod precursor cells in mouse retinal development. *J Neurosci.* 2011; 31(31):11118–11125.
29. Mears AJ, et al. Nrl is required for rod photoreceptor development. *Nat Genet.* 2001;29(4):447–452.
30. Oh EC, Khan N, Novelli E, Khanna H, Strettoi E, Swaroop A. Transformation of cone precursors to functional rod photoreceptors by bZIP transcription factor NRL. *Proc Natl Acad Sci U S A.* 2007; 104(5):1679–1684.
31. Freund CL, et al. Cone-rod dystrophy due to mutations in a novel photoreceptor-specific homeobox gene (CRX) essential for maintenance of the photoreceptor. *Cell.* 1997;91(4):543–553.
32. Swaroop A, et al. Leber congenital amaurosis caused by a homozygous mutation (R90W) in the homeodomain of the retinal transcription factor CRX: direct evidence for the involvement of CRX in the development of photoreceptor function. *Hum Mol Genet.* 1999;8(2):299–305.
33. Swain PK, et al. Mutations in the cone-rod homeobox gene are associated with the cone-rod dystrophy photoreceptor degeneration. *Neuron.* 1997;19(6):1329–1336.
34. Nichols LL 2nd, et al. Two novel CRX mutant proteins causing autosomal dominant Leber congenital amaurosis interact differently with NRL. *Hum Mutat.* 2010;31(6):E1472–E1483.
35. Huang L, et al. CRX variants in cone-rod dystrophy and mutation overview. *Biochem Biophys Res Commun.* 2012;426(4):498–503.
36. Daniele LL, et al. Cone-like morphological, molecular, and electrophysiological features of the photoreceptors of the Nrl knockout mouse. *Invest Ophthalmol Vis Sci.* 2005;46(6):2156–2167.
37. Roger JE, et al. Preservation of cone photoreceptors after a rapid yet transient degeneration and remodeling in cone-only Nrl$^{-/-}$ mouse retina. *J Neurosci.* 2012;32(2):528–541.
38. Solovei I, et al. Nuclear architecture of rod photoreceptor cells adapts to vision in mammalian evolution. *Cell.* 2009;137(2):356–368.
39. Cheng H, Khanna H, Oh EC, Hicks D, Mitton KP, Swaroop A. Photoreceptor-specific nuclear receptor NR2E3 functions as a transcriptional activator in rod photoreceptors. *Hum Mol Genet.* 2004; 13(15):1563–1575.
40. Peng GH, Ahmad O, Ahmad F, Liu J, Chen S. The photoreceptor-specific nuclear receptor Nr2e3 interacts with Crx and exerts opposing effects on the transcription of rod versus cone genes. *Hum Mol Genet.* 2005;14(6):747–764.
41. Brooks MJ, Rajasimha HK, Swaroop A. Retinal transcriptome profiling by directional next-generation sequencing using 100 ng of total RNA. *Methods Mol Biol.* 2012;884:319–334.
42. Ozawa Y, et al. Downregulation of STAT3 activation is required for presumptive rod photoreceptor cells to differentiate in the postnatal retina. *Mol Cell Neurosci.* 2004;26(2):258–270.
43. Ueki Y, Wang J, Chollangi S, Ash JD. STAT3 activation in photoreceptors by leukemia inhibitory factor is associated with protection from light damage. *J Neurochem.* 2008;105(3):784–796.
44. Kautzmann MA, Kim DS, Felder-Schmittbuhl MP, Swaroop A. Combinatorial regulation of photoreceptor differentiation factor, neural retina leucine zipper gene NRL, revealed by in vivo promoter analysis. *J Biol Chem.* 2011;286(32):28247–28255.
45. Terrell D, et al. OTX2 and CRX rescue overlapping and photoreceptor-specific functions in the Drosophila eye. *Dev Dyn.* 2012;241(1):215–228.
46. Jia L, et al. Retinoid-related orphan nuclear receptor ROR{beta} is an early-acting factor in rod photoreceptor development. *Proc Natl Acad Sci U S A.* 2009; 106(41):17534–17539.
47. Rivolta C, Berson EL, Dryja TP. Dominant Leber congenital amaurosis, cone-rod degeneration, and retinitis pigmentosa caused by mutant versions of

the transcription factor CRX. *Hum Mutat*. 2001; 18(6):488–498.

48. Silva E, Yang JM, Li Y, Dharmaraj S, Sundin OH, Maumenee IH. A CRX null mutation is associated with both Leber congenital amaurosis and a normal ocular phenotype. *Invest Ophthalmol Vis Sci*. 2000; 41(8):2076–2079.

49. Chen S, et al. Functional analysis of cone-rod homeobox (CRX) mutations associated with retinal dystrophy. *Hum Mol Genet*. 2002;11(8):873–884.

50. Cideciyan AV, et al. Centrosomal-ciliary gene CEP290/NPHP6 mutations result in blindness with unexpected sparing of photoreceptors and visual brain: implications for therapy of Leber congenital amaurosis. *Human Mutat*. 2007;28(11):1074–1083.

51. Homma K, et al. Developing rods transplanted into the degenerating retina of crx-knockout mice

exhibit neural activity similar to native photoreceptors. *Stem Cells*. 2013;31(6):1149–1159.

52. Lamba DA, Gust J, Reh TA. Transplantation of human embryonic stem cell-derived photoreceptors restores some visual function in Crx-deficient mice. *Cell Stem Cell*. 2009;4(1):73–79.

53. Roger JE, Nellissery J, Kim DS, Swaroop A. Sumoylation of bZIP transcription factor NRL modulates target gene expression during photoreceptor differentiation. *J Biol Chem*. 2010;285(33):25637–25644.

54. Priya RR, Rajasimha HK, Brooks MJ, Swaroop A. Exome sequencing: capture and sequencing of all human coding regions for disease gene discovery. *Methods Mol Biol*. 2012;884:335–351.

55. Li H, Durbin R. Fast and accurate long-read alignment with Burrows-Wheeler transform. *Bioinformatics*. 2010;26(5):589–595.

56. Li H, et al. The Sequence Alignment/Map format and SAMtools. *Bioinformatics*. 2009;25(16):2078–2079.

57. Wang K, Li M, Hakonarson H. ANNOVAR: functional annotation of genetic variants from high-throughput sequencing data. *Nucleic Acids Res*. 2010;38(16):e164.

58. Roger J, et al. Involvement of Pleiotrophin in CNTF-mediated differentiation of the late retinal progenitor cells. *Dev Biol*. 2006;298(2):527–539.

59. Matsuda T, Cepko CL. Electroporation and RNA interference in the rodent retina in vivo and in vitro. *Proc Natl Acad Sci U S A*. 2004;101(1):16–22.

60. Hao H, et al. The transcription factor neural retina leucine zipper (NRL) controls photoreceptor-specific expression of myocyte enhancer factor Mef2c from an alternative promoter. *J Biol Chem*. 2011; 286(40):34893–34902.